ACS APPLIED MATERIALS & INTERFACES

Research Article

www.acsami.org

Phase Stabilization of Al:HfO_2 Grown on $In_xGa_{1-x}As$ Substrates (x = 0, 0.15, 0.53) via Trimethylaluminum-Based Atomic Layer Deposition

Elena Cianci,[†,§] Alessandro Molle,*[,†,§] Alessio Lamperti,[†] Claudia Wiemer,[†] Sabina Spiga,[†] and Marco Fanciulli[†,‡]

[†]Laboratorio MDM, IMM-CNR, Via C. Olivetti 2, 20864 Agrate Brianza (MB), Italy

[‡]Dipartimento di Scienza dei Materiali, Università degli studi di Milano Bicocca, 20126 Milano, Italy

Supporting Information

ABSTRACT: Al:HfO_2 is grown on III−V compound substrates by atomic layer deposition after an in situ trimethylaluminum-based preconditioning treatment of the III−V surface. After post-deposition rapid thermal annealing at 700 °C, the cubic/tetragonal crystalline phase is stabilized and the chemical composition of the stack is preserved. The observed structural evolution of Al:HfO_2 on preconditioned III−V substrates shows that the in-diffusion of semiconductor species from the substrate through the oxide is inhibited. Al-induced stabilization of the Al:HfO_2 crystal polymorphs up to 700 °C can be used as a permittivity booster methodology with possibly important implications in the stack scaling issues of high-mobility III−V based logic applications.

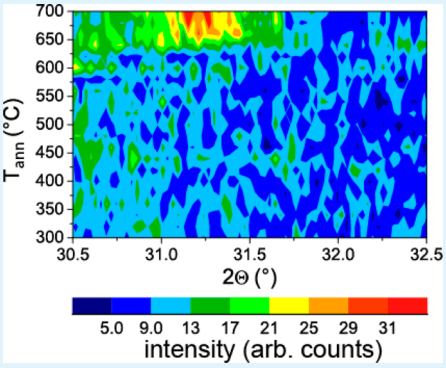

KEYWORDS: *phase stabilization, high-k dielectrics, trimethyl-aluminum, atomic layer deposition*

INTRODUCTION

HfO_2 is known to be polymorphic; i.e., monoclinic, cubic, and tetragonal phases are observed at atmospheric pressure and different temperatures. HfO_2 easily crystallizes in a polycrystalline monoclinic phase during deposition or upon annealing at temperature <500 °C, while tetragonal or cubic HfO_2 exists above 1670 and 2200 °C, respectively.[1] The orthorhombic phase is also predicted at high pressure conditions.[2] In general, the crystalline or amorphous structure of thin dielectric films can inherently affect their dielectric properties. In case of HfO_2 the dielectric constant strongly depends on its crystallographic phase, the cubic and tetragonal phases being predicted to have a much higher permittivity ($\kappa \sim 29$ and ~ 70, respectively) than that of amorphous or monoclinic ones ($\kappa \sim 16$).[3,4] This has made phase stabilized HfO_2-based oxides very attractive for applications in ultrascaled logic and memory devices. An efficient route to stabilize metastable phases relies on the artificial inclusion of a small amount of foreign atoms inside the high κ oxide matrix so as to favor the crystallization in cubic (c) and/or tetragonal (t) polymorphs at moderately low temperatures. Indeed, the dopant incorporation into HfO_2 has been predicted to be effective for phase stabilization,[5] and it has been demonstrated for several doping elements.[6−11] Al doping has also been exploited for HfO_2 phase engineering, therein obtaining a higher permittivity and lower leakage current over the conventional binary oxide.[12−14] In addition to high-κ dielectrics engineering, the implementation of high carrier mobility III−V compound semiconductors in advanced gate stack structures is considered a viable root for pushing metal oxide semiconductor field effect transistor (MOSFET) scaling to the end of the current technology generation.[15] Coupling high-κ dielectrics with III−V channels still represents a challenge due to the chemical and electronic instability of the oxide/semiconductor interface.[16] Atomic layer deposition (ALD) of Al_2O_3 has been successfully employed in controlling surface oxidation effects on III−Vs in order to achieve a low amount of interface states and electrically unpinned interfaces,[17−20] as a consequence of the "clean-up" effect,[21,22] namely, the reducing effect of the Al precursor trimethylaluminum [$Al_2(CH_3)_2$, conventionally denoted as TMA] on the III−V surface oxides. In this respect, incorporation of an ALD-grown Al_2O_3 control layer sandwiched in between HfO_2 and the III−V substrate or fabrication of Al_2O_3/HfO_2 nanolaminates have been proposed as solutions to design III−V friendly high-κ dielectrics with improved electrical and insulating properties.[23−27]

In this work we report on the ALD process of Al-doped HfO_2 (Al:HfO_2) developed on SiO_2/Si and transferred on III−V substrates, with in situ preconditioning surface treatment by few TMA-based Al_2O_3 cycles, resulting in a robust stack where the Al:HfO_2 film can be stabilized, upon proper thermal treatment, in the metastable c/t polymorph. Besides the technological benefit in terms of ultrascaled post-Si CMOS devices, our focus is to develop an ALD process to manufacture

Received: December 6, 2013
Accepted: February 10, 2014
Published: February 10, 2014

   dx.doi.org/10.1021/am405617q | ACS Appl. Mater. Interfaces 2014, 6, 3455−3461

an Hf-based oxide, enabling low temperature phase stabilization by aluminum doping, thus opening a viable route for a III−V compatible permittivity engineering. After an Experimental Section where the techniques and the methods are described, the results will be presented and discussed in a dedicated section. For clarity of the reading, the latter section is organized as follows. First, we make evidence of the crystallization onset in Al:HfO_2 (both on SiO_2/Si and on III−V compound substrates) at significantly lower temperature than the purely undoped HfO_2 by means of X-ray diffraction analysis. Then, we will focus on phase stabilization of Al:HfO_2 on $In_{0.15}Ga_{0.85}As$ substrates in terms of interface chemistry and chemical stability of the stacked structures. In this framework, we bring preliminary evidence of an enhancement of the oxide permittivity upon phase stabilization by means of electrical characterization of the relevant MOS capacitors. Finally, the compositional integrity of the Al:HfO_2/$In_{0.15}Ga_{0.85}As$ is scrutinized in order to assess the activation of in-diffusion from the substrate inside the oxide.

EXPERIMENTAL SECTION

Al:HfO_2 films are grown at 300 °C by thermal ALD in a flow type hot wall Savannah 200 (Cambridge Nanotech) reactor, employing TMA as aluminum source and the hafnium cyclopentadienyl compound ($MeCp_2HfMe(OMe)$ denoted as HfD-04, Sigma Aldrich) as Hf precursor and using H_2O as oxygen source. TMA and water are kept at room temperature, while the HfD-04 cylinder is kept at 110 °C to ensure high enough vapor pressure; precursors are driven by 20 sccm N_2 carrier gas into the reactor chamber at 0.6 Torr pressure. The incorporation of aluminum in the HfO_2 matrix is obtained by alternating the ALD cycles optimized for the growth of the binary oxides Al_2O_3 and HfO_2, respectively, and the aluminum content in the HfO_2 film can be tuned by varying the ALD Al_2O_3 to HfO_2 cycle ratio. Films are deposited onto 4.5 nm SiO_2/Si as nonreactive reference substrates and on $In_xGa_{1-x}As$ substrates with variable In(Ga) concentration (x = 0, 0.15, 0.53). p-type $In_{0.15}Ga_{0.85}As$ and p-type GaAs surfaces are cleaned of their native oxides using NH_4OH 25% and passivated in $(NH_4)_2S$ 20% aqueous solution while n-type $In_{0.53}Ga_{0.47}As$ is decapped from an As protective layer by thermal desorption in ultrahigh vacuum environment and then treated in 20% $(NH_4)_2S$ solution before being loaded in the ALD reactor.[28] In order to reach a similar stable interface to that assessed for Al_2O_3/III−V stacks, the ALD process starts with an in situ preconditioning by five ALD cycles of Al_2O_3, with TMA as the first 0.5-s-long pulse to ensure the reported "clean up" effect.[21,28] Then Al:HfO_2 films are deposited setting the Al_2O_3:HfO_2 ALD cycle ratio to 1:12 which results in Al:HfO_2 atomic composition of 4.4% Al, 34.8% Hf, and 60.8% oxygen as detected by X-ray photon electron spectroscopy (XPS),[14,29] independently of the starting substrate. Details of the ALD process are reported in the Supporting Information and can be also found in ref 29. Nominal film thickness is calibrated with spectroscopic ellipsometry. Two different heating procedures have been performed, slow annealing during in situ high temperature X-ray diffraction (HTXRD) monitoring (from room temperature to 600 °C: 50 °C/min, from 600 °C until final temperature via a ceramic heater, 20 °C/min and 30 s of measurement time each 10 °C); fast rapid thermal annealing (RTA: 700 °C in 30 s under N_2 rich pressure via a heating lamp). HTXRD has been performed with a laboratory instrument equipped with a four-circle goniometer and a position sensitive detector, and a heating stage able to reach temperature as high as 1100 °C was utilized to identify the oxide crystallization onset as a function of the annealing temperature or as ex situ diagnostic on RTA treated samples. The chemical details of the interface and the compositional depth profiling were investigated by ex situ XPS and time-of-flight secondary ion mass spectroscopy (ToF-SIMS), respectively. The stacked structures were assessed by ex situ X-ray reflectivity (XRR). Preliminary electrical characterization has been performed on MOS capacitors incorporating Au electrodes with an effective area of 0.385 mm^2, Al:HfO_2 gate dielectrics, and p-type $In_{0.15}Ga_{0.85}As$ substrates by means of Agilent E4980A meter.

RESULTS AND DISCUSSION

Phase Stabilization: In Situ Diffraction Analysis. The structural evolution of Al:HfO_2 with increasing temperatures has been investigated using in situ HTXRD monitoring. A first relevant effect of the Al incorporation is that the as-deposited films are amorphous regardless of the substrates, therein manifesting a clear discrepancy from the deposition of pure HfO_2 at 300 °C which mostly crystallizes in the monoclinic phase.[30]

Structural changes of Al:HfO_2 films (with nominal thickness of 24 nm) deposited on SiO_2/Si reference substrates are studied as a function of temperature (in ambient pressure), from the deposition temperature (300 °C) to 700 °C using a heating rate of 20 °C/min and a soaking time of 30 s. The onset temperature for the crystallization is observed to be around 640−660 °C as results from in situ HTXRD scans piled up in Figure 1a as a function of the temperature. The observed

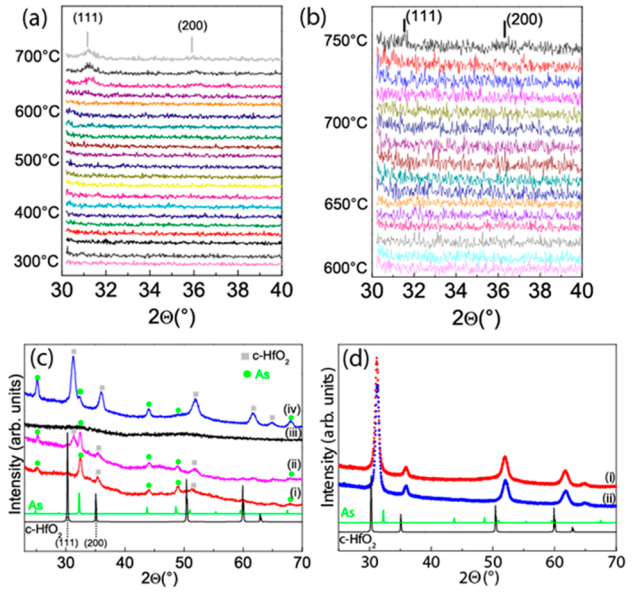

Figure 1. (a) In situ HTXRD snapshots of 24 nm (nominally) thick Al:HfO_2 on SiO_2/Si at 20 °C/min with increasing measurement temperature. The onset of phase crystallization is identified by the emergence of a (111) peak at T = 640 °C. (b) In situ HTXRD snapshots of 15 nm (nominally) thick Al:HfO_2 on GaAs at 20 °C/min with increasing measurement temperature. (c) Ex situ highly resolved XRD patterns of 15 nm Al:HfO_2 films taken at room temperature after long annealing at (i) 700 °C on $In_{0.15}Ga_{0.58}As$, (ii) 710 °C on $In_{0.53}Ga_{0.47}As$, and (iii) 750 °C on GaAs. (d) Ex situ highly resolved XRD patterns of 19 nm Al:HfO_2 films after RTA at 700 °C on (i) $In_{0.15}Ga_{0.85}As$ and (ii) SiO_2/Si. The diffraction patterns of cubic HfO_2 and of As are reported for comparison.[31]

diffraction peaks in Figure 1a are consistent with the reflection from (111) and (200) planes in a stabilized c/t crystalline phase of the Al:HfO_2. A more incisive view of the emerging crystallization can be deduced from the diffraction map reported in Figure S1 of the Supporting Information. It must be emphasized that a moderate Al incorporation (4.4% according to the XPS compositional check) in the HfO_2 matrix is enough to significantly decrease the crystallization temper-

dx.doi.org/10.1021/am405617q | ACS Appl. Mater. Interfaces 2014, 6, 3455−3461

ature of cubic/tetragonal (pure) HfO_2 (i.e., temperatures higher than 1500 °C and high pressure) and to stabilize this phase upon cooling back to room temperature, thus making it suitable to low temperature integration on substrates (such as the III−V compounds) that are sensitive to a large process thermal budget. An increase of the cycle ratio from 1:12 to 1:6, with a correspondingly increased Al concentration from 4.4% to 7.0%, has been observed to shift the crystallization onset to higher temperatures, in agreement with Wang and Ekerdt.[31] Therefore, the here reported 1:12 cycle ratio was assumed to be a good trade-off between achieving a crystallization onset low enough not to impact the III−V compound integrity and growing a scalable Al:HfO_2 film.

We adopt a similar procedure to monitor the onset in Al:HfO_2 film crystallization when using III−V compounds as substrates. Since those substrates are expected to be less stable than SiO_2, in the HTXRD analysis diffraction patterns have been acquired at narrower temperature increments (i.e., every 10 °C), from 600 °C up to a maximum temperature in between 660 and 750 °C (depending on the substrate), and after heating up to 600 °C with 50 °C/min rate and a soaking time of 30 s. The in situ HTXRD analysis performed on a 15-nm-thick Al:HfO_2 grown on a GaAs(001) substrate is shown in Figure 1b. Despite the low signal-to-noise ratio (most probably due to the physically smaller size of the sample), the crystallization temperature turns out to be sensibly higher (750 °C) than that measured when using the SiO_2/Si substrate. This fact is more clearly elucidated by the ex situ highly resolved XRD scan on the latter sample taken in the XRD sample holder upon long annealing at 660 and 750 °C (see respectively scans (iii) and (iv) in Figure 1c). Heating at 600 °C actually results in no diffraction pattern, whereas (111) and (200) diffraction peaks of the *c*/*t* phase[32] can be observed after heating at 750 °C. Conversely, from the ex situ XRD scans (i) and (ii) in Figure 1c, crystallization of the Al:HfO_2 on the two other III−V compounds, $In_{0.15}Ga_{0.85}As$(001) and $In_{0.53}Ga_{0.47}As$(001), is observable after heating at intermediate temperatures of 700 and 710 °C, respectively, namely in between the case of the GaAs and of the SiO_2/Si substrate. Patterns in Figure 1c are highly integrated XRD scans recorded from Al:HfO_2 on III−V compound substrates at room temperature after the in situ analysis (stopped at the crystallization temperature) in order to reduce the signal-to-noise ratio for a more accurate identification of the diffraction peaks (such an accuracy was not possible during the in situ analysis because it could have caused interface instability with the III−V substrate due to an intolerably high thermal budget). The observed diffraction peaks can be unambiguously assigned to *c*/*t* HfO_2 polymorphs (see square marked peaks in Figure 1c) and to crystallized As (see circle marked peaks in Figure 1c). The latter evidence can be related to the formation of As precipitates in III−V substrates after the long-time cumulative annealing[33] borne along the HTXRD measurement. Therefore two competitive processes take place in the thermal ramp of the HTXRD measurement, i.e., the thermally activated Al:HfO_2 film crystallization and the kinetically driven As diffusion and precipitation.

Phase Stabilization: Rapid Thermal Processing. A rapid thermal annealing (RTA) process has been performed by ramping the temperature immediately up to 700 °C in 30 s inside a N_2-rich environment in order to suppress As crystallization (kinetic in nature) and to achieve the oxide film crystallization without significant As clustering. The postgrowth RTA results in the XRD patterns shown in Figure 1d for Al:HfO_2 films deposited on $In_{0.15}Ga_{0.85}As$ and SiO_2/Si. No As precipitation is observed in the $In_{0.15}Ga_{0.85}As$ substrate, and the same phase stabilization with the same preferential orientation takes place on both films, irrespectively of the substrate, as results from the close analogy between the measured diffraction pattern of RTA treated Al:HfO_2 and the tabulated pattern of c-HfO_2.[32] It can be noticed that the Al:HfO_2 peaks in Figure 1c and Figure 1d have mutually different intensity ratios. According to ab initio calculations of the cubic and tetragonal HfO_2 phases,[34] the energy difference between the (111) and (100) surfaces is extremely small, and it dramatically depends on the details of the termination (i.e., O, O−O, or Hf). Therefore, such a delicate balance between the two planes can be significantly influenced by the constraints of our experimental procedures, including the Al incorporation as well as the annealing treatments. The observed discrepancy in terms of (111)/(200) peak ratio between Figure 1c and Figure 1d can be thus tentatively associated with the As precipitation which is activated during the in situ HTXRD monitoring. In detail, the role of the As precipitation in the oxide phase stabilization can be elucidated in its phenomenological character by the following facts. First, from a more careful comparison among scans (i), (ii), and (iii) in Figure 1c, the (111)/(200) intensity ratio increases with increasing annealing temperatures. Second, if we take into account the in situ HTXRD spectra for the Si/SiO_2 substrate in Figure 1a, at 640 °C the (111) and (200) reflections have similar intensity values, whereas at higher temperatures, the (111) intensity increases and the (200) peak becomes less significant, and finally at 700 °C, no (200) intensity is registered. Moreover, the (111)/(200) intensity ratio measured on the $In_{0.15}Ga_{0.85}As$ substrate after long annealing at 700 °C (Figure 1c) resembles the one observed on the Si/SiO_2 substrate after long annealing at 640 °C (Figure 1 a). Third, when As precipitation does not occur (upon RTA, see XRD scans in Figure 1d), XRD patterns of Al:HfO_2 deposited on Si/SiO_2 and on $In_{0.15}Ga_{0.85}As$ exhibit the same features upon RTA at 700 °C. These facts suggest that the detected As precipitation delays the Al:HfO_2 crystallization along some preferential crystalline surfaces during the prolonged annealing of the in situ HTXRD measurement.

Arsenic Stability at the Interface. From the diffraction analysis, the role of As at the interface is quite delicate as it can undergo thermally driven precipitation. Therefore, the As stability at the interface has been assessed by XPS diagnostic of the As 3d core level photoemission lines of a 3 nm-thick Al:HfO_2 film grown on $In_{0.15}Ga_{0.85}As$ prior to and after RTA, respectively reported in Figure 2a,b. Deconvolution of both As 3d lines involves three physically different components in the limit of the XPS resolution, i.e., the Hf $5p_{1/2}$ peak at binding energy BE = 40.0 eV, the As 3d peak at BE = 40.9 eV from the substrate (denoted as As^S), and an additional As-related peak at BE = 41.7 eV (denoted as As*). The origin of the As* component can be associated with the presence of AsO_x suboxide species,[35,36] As−As homopolar bonding,[35−37] As−S bonding,[28,38] or a convolution of all these facts. Nonetheless such a component is reduced in its intensity after RTA. No As_2O_3 or As_2O_5 related component can be deduced from the measured lines for BE > 43.5 eV.[37] From a qualitative comparison between the As 3d lines in Figure 2a,b, no significant modification of the As chemical environment can be deduced upon RTA treatment. More quantitatively, the relative intensity of the components changes upon RTA. In particular, a

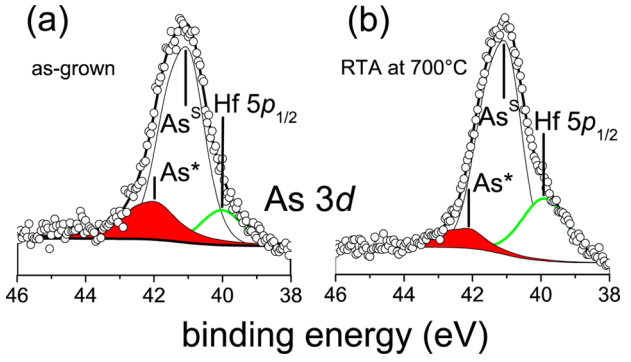

Figure 2. As 3d XPS line of 3 nm-thick Al:HfO_2 film grown on $In_{0.15}Ga_{0.85}As$: as-grown (a), upon RTA at 700 °C (b). The line deconvolution consists of the Hf $5p_{1/2}$ peak, the As 3d peak from the substrate (As^S), and the extra-component As*. XPS intensities are normalized to the measured maxima in a unity scale. Details on the deconvolution procedure are reported in the Supporting Information.

smaller As^S/Hf $5p_{1/2}$ intensity ratio can be inferred which is consistent with an annealing-induced thickness reduction of the oxide.

Stack Structure Characterization. The X-ray reflectivity (XRR) analysis in Figure 3 is intended to assess the presumed

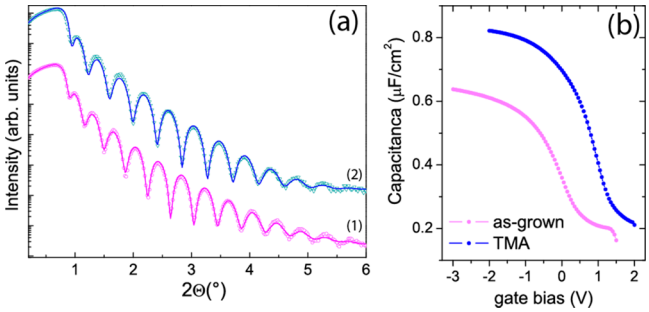

Figure 3. (a) XRR scans (open dots) and fitting curves (lines) for Al:HfO_2 on $In_{0.15}Ga_{0.85}As$ (with nominal thickness of 19 nm), as-deposited (a) and after RTA at 700 °C (b). (b) Capacitance–voltage curves taken at 100 kHz from MOS capacitors incorporating the Al:HfO_2 films as described in panel (a).

thickness reduction of the oxide and to provide tips of the Al:HfO_2/III–V stack stability upon RTA. From the XRR data recorded on a (nominally) 19-nm-thick Al:HfO_2 on $In_{0.15}Ga_{0.85}As$ substrate, the stack can be modeled by accounting for an interfacial region in between the film and the substrate, as due to the Al_2O_3 preconditioning cycles.[29] According to Table 1, this interfacial region is not significantly affected by the RTA process (the thickness is comprised in between 1.9 and 2.0 nm), except for a slightly increased roughening (from 0.3 to 0.5 nm after RTA). RTA at 700 °C also induces a densification of the film corresponding to an increase of the electronic density of the order of 5% and a decrease in the layer thickness of 7% in agreement with the smaller As^S/Hf $5p_{1/2}$ XPS intensity ratio in Figure 2b. In detail, the Al:HfO_2 region has a thickness of 20.9 nm on the as-deposited film which is thinned down to 19.5 nm upon RTA. In the attempt to assess the effect of phase stabilization in the oxide permittivity, a preliminary electrical characterization of the MOS capacitors incorporating amorphous Al:HfO_2 (as-grown) and *c*/*t* Al:HfO_2 (RTA-treated) as dielectric gates and p-type $In_{0.15}Ga_{0.85}As$ as substrate has been performed. In Figure 3b the capacitance–voltage curves, recorded at 100 kHz, are reported for both MOS capacitors upon correction on the series resistance and normalization on the electrode area. The curves are mutually shifted in the bias scale. This fact can be ascribed to a different amount of fixed charge in the two dielectric stacks. Nonetheless, it must be emphasized that the accumulation capacitance in case of the *c*/*t* Al:HfO_2 is significantly higher than that of the amorphous counterpart thus hinting at a sensible enhancement of the inherent permittivity. On the basis of the structural parameters listed in Table 1 and assuming an Al_2O_3-rich interface layer with permittivity of 6.9,[29] the permittivity values extracted from the measured accumulation capacitance amount to 19.0 (consistently with ref 29) and to 24.9, respectively, for the amorphous and *c*/*t* Al:HfO_2, thus indicating an increase of about 31% upon phase stabilization. Further characterization needed to assess the electrical quality of the MOS capacitors is beyond the scope of the present study.

Table 1. XRR Deduced Thickness, Roughness, and Electron Density of As-Deposited and Annealed Al:HfO_2 on $In_{0.15}Ga_{0.85}As$

	thickness ± 0.1 (nm)		roughness ± 0.1 (nm)		electron density ± 0.05 ($e^-/Å^3$)	
layer	AS dep	RTA	As dep	RTA	As dep	RTA
Al:HfO_2	20.9	19.5	0.8	0.8	2.35	2.47
interlayer	1.9	2.0	0.3	0.5	1.31	1.31
$In_{0.15}Ga_{0.85}As$	30	30	0.3	0.5	0.3	0.5

The reported evidence concurs to support the two following facts: (a) the developed TMA-based ALD process results in stable Al:HfO_2/III–V stacks; (b) the so-grown Al:HfO_2/III–V stacks undergo phase transition upon RTA at high temperature without altering their own constitution. To consolidate these findings, we speculate that the initial Al_2O_3 cycles onto the III–V substrate create a stable interface that blocks or at least largely attenuates the film-to-substrate reactivity, enabling the transfer of the Al:HfO_2 film onto III–V substrates with the same properties of those developed on SiO_2/Si. Therefore, phase stabilization is exclusively attributed to the incorporation of Al in the HfO_2 films after annealing, regardless of the substrate reactivity.

Depth Profiling Characterization. Although As crystallization is not fast enough to occur during the RTA process, RTA induced in-diffusion from the substrate through the interface cannot be apodictically ruled out from the previous data. In this respect, a deeper insight into the interface stability of the stack structure can be achieved by means of ToF-SIMS measurements. Figure 4a,b show ToF-SIMS depth profiles of 19 nm (nominally)-thick Al:HfO_2 on preconditioned $In_{0.15}Ga_{0.85}As$, as deposited and after RTA at 700 °C in N_2 for 30 s. HfO and AlO_2 signals are constant across the thickness direction in the limit of the ToF-SIMS resolution, thus evidencing the uniform compositional distribution of the film. At the interface with the $In_{0.15}Ga_{0.85}As$ substrate a higher AlO_2 signal is detected that can be related to the preconditioning TMA + H_2O cycles on the $In_{0.15}Ga_{0.85}As$ surface and hence to the existence of a Al_2O_3-rich interface layer. The same number of Al_2O_3 cycles onto the 4.5-nm-thick SiO_2/Si surface results in a less pronounced peak in the AlO_2 signal[29] compared to that on the III–V substrate, then giving proof of the enhanced TMA reactivity with the semiconductor native oxides (especially the As oxides).[35,36] The presence of In, Ga, and As related oxides

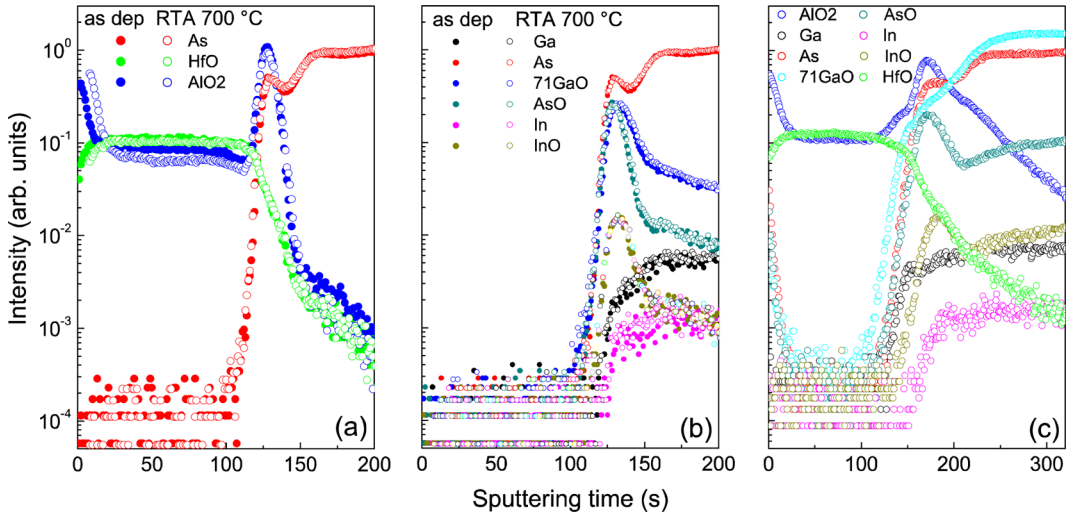

Figure 4. ToF-SIMS depth profiles (with 0.5 keV Cs^+ sputtering beam) of 19 nm-thick Al:HfO_2 on top of p-$In_{0.15}Ga_{0.85}As$, of as deposited (full dots) and annealed (RTA at 700 °C) (open dots). In panel (a) HfO and AlO_2 signals from the film and As signal from the substrate are reported, while in panel (b) signals from the substrates are evidenced. Profiles are aligned on Al:HfO_2/$In_{0.15}Ga_{0.85}As$ interface, i.e., AlO_2 (or euqivalently AsO) maximum intensity. (c) Extensive ToF-SIMS depth profiling of 3 nm-thick Al:HfO_2/$In_{0.15}Ga_{0.85}As$ upon annealing at 700 °C (the scale is identical to panels (a) and (b) because a 0.25 keV Cs^+ sputtering beam was used).

cannot be ruled out from the Al_2O_3-rich interfacial region, in the limit of the in-depth resolution (<3 Å) and sensitivity (lower than one part percent) of the technique.

To this regard, while no As oxides are recognized by XPS (see Figure 2), marginal formation of In−O and Ga−O bonding can be inferred from the In 3d and Ga 3s XPS lines (see Supporting Information) despite the spectra resolution being quite poor as due to the relatively low In amount in the $In_{0.15}Ga_{0.85}As$ and to the difficulty in detecting other more conventional Ga-related XPS lines. RTA at 700 °C has no significant effect on the chemical profile of the film and the interface.

The interfacial region between the Al:HfO_2 film and the substrate remains well-defined, and no significant broadening is detected and no in-diffusion of substrate elements into the high-κ oxide film is observed. This corroborates the hypothesis that the initial Al_2O_3 cycles create a stable interfacial region, preventing in-diffusion of elemental species from the substrate into the film as well as the interdiffusion of external oxygen through the film within the used thermal budget.[39,40] It can be argued that interface instabilities such as thermally induced interdiffusion of mobile In from the substrate may be activated when the Al:HfO_2 is reduced to a few nanometers,[41] namely, in a range of interest for ultimately scaled dielectric gates. To elucidate this aspect, an extended ToF-SIMS depth profiling analysis (using 0.25 keV Cs^+ sputtering beam) is reported in Figure 4c for a 3-nm-thick Al:HfO_2 film grown on $In_{0.15}Ga_{0.85}As$ upon RTA at 700 °C. No significant tail of the semiconductor-related signals can be deduced throughout the oxide region from the profiles in Figure 4c, ruling out massive interdiffusion of a specific semiconductor according to the extremely high sensitivity of the ToF-SIMS measurement. These facts demonstrate that the developed process not only leads to phase stabilization but also prevents in-diffusion from the substrate even when the oxide thickness is limited to 3 nm.

CONCLUSIONS

Crystallization in the cubic/tetragonal high-κ HfO_2 polymorphs of ALD Al:HfO_2 deposited on both SiO_2/Si and III−V substrates is observed after annealing in the 700−750 °C (depending on the III−V compound substrate), and it is univocally ascribed to the Al incorporation by TMA pulse intercalation in the ALD sequence, irrespectively of the chemical specificity and the surface reactivity of the substrate. The TMA-based preconditioning treatment provides a chemically stable interface with III−V surface even after phase stabilization of the overlying Al:HfO_2 film. The present outcomes validate a methodology for artificially forcing crystal phase stabilization in an oxide matrix providing new tips for permittivity engineering of high-κ materials even on highly reactive III−V substrates.

ASSOCIATED CONTENT

Supporting Information

(a) Details on the substrates and the oxide growth; (b) details on the experimental techniques (where the XPS deconvolution approach and the intensity ratios of the deconvoluting components in the As 3d XPS lines are specified); and (c) additional data supporting the interface stability upon annealing. This material is available free of charge via the Internet at http://pubs.acs.org.

AUTHOR INFORMATION

Corresponding Author

*E-mail: alessandro.molle@mdm.imm.cnr.it (A.M.).

Author Contributions

[§]These authors (E.C. and A.M.) contributed to this work equally.

Author Contributions

A.M., S.S., and M.F. conceived the idea. E.C. managed the ALD and postgrowth processing. C.W. performed the XRD and XRR measurements. A.L. performed the ToF-SIMS measurements. A.M. performed the XPS characterization. S.S. and M.F. conducted the project work. All authors concur in the scientific discussion and in the manuscript writing.

Notes

The authors declare no competing financial interest.

■ ACKNOWLEDGMENTS

The authors acknowledged the ARAMIS project in collaboration with IMEC (Belgium) for the partial supply of the III−V substrates.

■ ABBREVIATIONS

TMA, trimethyl-aluminum

■ REFERENCES

(1) Massalski, T. B. *Binary alloy phase diagrams*, 2nd ed.; ASM International, Materials Park, OH, 1990.
(2) Kang, J.; Lee, E.-C.; Chang, K. J. First-principles study of the structural phase transformation of hafnia under pressure. *Phys. Rev. B* **2003**, *68*, 054106.
(3) Zhao, X.; Vanderbilt, D. First-principles study of structural, vibrational, and lattice dielectric properties of hafnium oxide. *Phys. Rev. B* **2002**, *65*, 233106.
(4) Ceresoli, D.; Vanderbilt, D. Structural and dielectric properties of amorphous ZrO_2 and HfO_2. *Phys. Rev. B* **2006**, *74*, 125108.
(5) Lee, C.-K.; Cho, E.; Lee, H.-S.; Hwang, C. S.; Han, S. First-principles study on doping and phase stability of HfO_2. *Phys. Rev. B* **2008**, *78*, 012102.
(6) Govindarajan, S.; Böscke, T. S.; Sivasubramani, P.; Kirsch, P. D.; Lee, B. H.; Tseng, H.-H.; Jammy, R.; Schröder, U.; Ramanathan, S.; Gnade, B. E. Higher permittivity rare earth doped HfO_2 for sub-45-nm metal−insulator−semiconductor devices. *Appl. Phys. Lett.* **2007**, *91*, 062906.
(7) Adelmann, C.; Sriramkumar, V.; Van Elshocht, S.; Lehnen, P.; Conard, T.; De Gendt, S. Dielectric properties of dysprosium- and scandium-doped hafnium dioxide thin films. *Appl. Phys. Lett.* **2007**, *91*, 162902.
(8) Tomida, K.; Kita, K.; Toriumi, A. Dielectric constant enhancement due to Si incorporation into HfO_2. *Appl. Phys. Lett.* **2006**, *89*, 142902.
(9) Kita, K.; Kyuno, K.; Toriumi, A. Permittivity increase of yttrium doped HfO_2 through structural phase transformation. *Appl. Phys. Lett.* **2005**, *82*, 102906.
(10) He, W.; Zhang, L.; Chan, D. S. H.; Cho, B. J. Cubic-Structured HfO_2 With Optimized Doping of Lanthanum for Higher Dielectric Constant. *IEEE Electron Dev. Lett.* **2009**, *30*, 623−625.
(11) Wiemer, C.; Lamagna, L.; Baldovino, S.; Perego, M.; Schamm-Chardon, S.; Coulon, P. E.; Salicio, O.; Congedo, G.; Spiga, S.; Fanciulli, M. Dielectric properties of Er−doped HfO_2 (Er∼15%) grown by atomic layer deposition for high-k gate stacks. *Appl. Phys. Lett.* **2010**, *96*, 182901.
(12) Park, P. K.; Kang, S.-W. Enhancement of dielectric constant in HfO_2 thin films by the addition of Al_2O_3. *Appl. Phys. Lett.* **2006**, *89*, 192905.
(13) Park, T. J.; Kim, J. H.; Jang, J. H.; Lee, C.-K.; Na, K. D.; Lee, S. Y.; Jung, H.-S.; Kim, M.; Han, S.; Hwang, C. S. Reduction of Electrical Defects in Atomic Layer Deposited HfO_2 Films by Al Doping. *Chem. Mater.* **2010**, *22*, 4175−4184.
(14) Congedo, G.; Wiemer, C.; Lamperti, A.; Cianci, E.; Molle, A.; Volpe, F. G.; Spiga, S. Atomic layer-deposited Al−HfO_2/SiO_2 bi-layers towards 3D charge trapping non-volatile memories. *Thin Solid Films* **2013**, *533*, 9−14.
(15) International Technological Roadmap for Semiconductor, 2011 Edition and 2012 Update. www.itrs.net, February 2014.
(16) Hinkle, C. L.; Vogel, E. M.; Ye, P. D.; Wallace, R. M. Interfacial chemistry of oxides on $In_xGa_{(1-x)}As$ and implications for MOSFET applications. *Curr. Opin. Solid State Mater. Sci.* **2011**, *15*, 188−207.
(17) Kim, E. J.; Chagarov, E.; Cagnon, J.; Yuan, Y.; Kummel, A. C.; Asbeck, P. M.; Stemmer, S.; Saraswat, K. C.; McIntyre, P. C. Atomically abrupt and unpinned Al_2O_3/$In_{0.53}Ga_{0.47}As$ interfaces: Experiment and simulation. *J. Appl. Phys.* **2009**, *106*, 124508.
(18) Melitz, W.; Kent, T.; Kummel, A. C.; Droopad, R.; Holland, M.; Thayne, I. Atomic imaging of atomic layer deposition oxide nucleation with trimethylaluminum on As-rich InGaAs(001) 2 × 4 vs Ga/In-rich InGaAs(001) 4 × 2. *J. Chem. Phys.* **2012**, *136*, 154706.
(19) Molle, A.; Lamagna, L.; Grazianetti, C.; Brammertz, G.; Merckling, C.; Caymax, M.; Spiga, S.; Fanciulli, M. Reconstruction dependent reactivity of As-decapped $In_{0.53}Ga_{0.47}As(001)$ surfaces and its influence on the electrical quality of the interface with Al_2O_3 grown by atomic layer deposition. *Appl. Phys. Lett.* **2011**, *99*, 193505.
(20) Grazianetti, C.; Molle, A.; Tallarida, G.; Spiga, S.; Fanciulli, M. Effect of Electric Dipoles on Fermi Level Positioning at the Interface between Ultrathin Al2O3 Films and Differently Reconstructed $In_{0.53}Ga_{0.47}As(001)$ Surfaces. *J. Phys. Chem. C* **2012**, *116*, 18746−18751.
(21) Hinkle, C. L.; Sonnet, A. M.; Vogel, E. M.; McDonnell, S.; Hughes, G. J.; Milojevic, M.; Lee, B.; Aguirre-Tostado, F. S.; Choi, K. J.; Kim, H. C.; Kim, J.; Wallace, R. M. GaAs interfacial self-cleaning by atomic layer deposition. *Appl. Phys. Lett.* **2008**, *92*, 071901.
(22) S. Klejna, S.; Elliott, S. First-Principles Modeling of the "Clean-Up" of Native Oxides during Atomic Layer Deposition onto III−V Substrates. *J. Phys. Chem. C* **2012**, *116*, 643−654.
(23) Suzuki, R.; Taoka, N.; Yokoyama, M.; Lee, S.; Kim, S. H.; Hoshii, T.; Yasuda, T.; Jevasuwan, W.; Maeda, T.; Ichikawa, O.; Fukuhara, N.; Hata, M.; Takenaka, M.; Takagi, S. 1-nm-capacitance-equivalent-thickness HfO_2/Al_2O_3/InGaAs metal-oxide-semiconductor structure with low interface trap density and low gate leakage current density. *Appl. Phys. Lett.* **2012**, *100*, 132906.
(24) Monaghan, S.; O'Mahony, A.; Cherkaoui, K.; O'Connor, É.; Povey, I. M.; Nolan, M. G.; O'Connell, D.; Pemble, M. E.; Hurley, P. K.; Provenzano, G.; Crupi, F.; Newcomb, S. B. Electrical analysis of three-stage passivated $In_{0.53}Ga_{0.47}As$ capacitors with varying HfO_2 thicknesses and incorporating an Al_2O_3 interface control layer. *J. Vac. Sci. Technol. B* **2011**, *29*, 01A807.
(25) Chu, L. K.; Merckling, C.; Alian; Dekoster, J.; Kwo, J.; Hong, M.; Caymax, M.; Heyns, M. Low interfacial trap density and sub-nm equivalent oxide thickness in $In_{0.53}Ga_{0.47}As$ (001) metal-oxide-semiconductor devices using molecular beam deposited HfO_2/Al_2O_3 as gate dielectrics. *Appl. Phys. Lett.* **2011**, *99*, 042908.
(26) Mahata, C.; Byun, Y.-C.; An, C.-H.; Choi, S.; An, Y.; Kim, H. Comparative Study of Atomic-Layer-Deposited Stacked (HfO_2/Al_2O_3) and Nanolaminated ($HfAlO_x$) Dielectrics on $In_{0.53}Ga_{0.47}As$. *ACS Appl. Mater. Interfaces* **2013**, *5*, 4195−4201.
(27) Lin, T. D.; Chang, Y. H.; Lin, C. A.; Huang, M. L.; Lee, W. C.; Kwo, J.; Hong, M. Realization of high-quality HfO_2 on $In_{0.53}Ga_{0.47}As$ by in-situ atomic-layer-deposition. *Appl. Phys. Lett.* **2012**, *100*, 172110.
(28) Lamagna, L.; Fusi, M.; Spiga, S.; Fanciulli, M.; Brammertz, G.; Merckling, C.; Meuris, M.; Molle, A. Effects of surface passivation during atomic layer deposition of Al_2O_3 on $In_{0.53}Ga_{0.47}As$ substrates. *Microelectron. Eng.* **2011**, *88*, 431−434.
(29) Molle, A.; Cianci, E.; Lamperti, A.; Wiemer, C.; Spiga, S.; Fanciulli, M. A viable route to enhance permittivity of gate dielectrics on $In_{0.53}Ga_{0.47}As(001)$: Trimethylaluminum-Based Atomic Layer Deposition of MeO_2 (Me═Zr, Hf). *ECS J. Solid State Sci. Technol.* **2013**, *2* (9), P395−P399.
(30) Spiga, S.; Driussi, F.; Lamperti, A.; Congedo, G.; Salicio, O. Effects of Thermal Treatments on the Trapping Properties of HfO2 Films for Charge Trap Memories. *Appl. Phys. Express* **2012**, *5*, 021102.
(31) Wang, T.; Ekerdt, J. G. Structure versus Thermal Stability: The Periodic Structure of Atomic Layer Deposition-Grown Al-Incorporated HfO2 Films and Its Effects on Amorphous Stabilization. *Chem. Mater.* **2011**, *23*, 1679−1885.
(32) Inorganic Crystal Structure Database, file 53033 for c-HfO_2 and file 158473 for As. Fach information zentrum, Karslruhe, 2013.
(33) Liliental-Weber, Z.; Lin, X. W.; Washburn, J.; Schaff, W. Rapid thermal annealing of low temperature GaAs layers. *Appl. Phys. Lett.* **1995**, *66*, 2086.
(34) Beltrán, J.; Muñoz, M. C.; Hafner, J. Structural, electronic and magnetic properties of the surfaces of tetragonal and cubic HfO_2. *New J. Phys.* **2008**, *10*, 063031.
(35) Tallarida, M.; Adelmann, C.; Delabie, A.; Van Elshocht, S.; Caymax, M.; Schmeisser, D. Surface chemistry and Fermi level

movement during the self-cleaning of GaAs by trimethyl-aluminum. *Appl. Phys. Lett.* **2011**, *99*, 042906.
(36) Brennan, B.; Zhernokletov, D. M.; Dong, H.; Kim, J.; Wallace, R. M. In situ surface pre-treatment study of GaAs and $In_{0.53}Ga_{0.47}As$. *Appl. Phys. Lett.* **2012**, *100*, 151603.
(37) Marchiori, C.; Kiewra, E.; Fompeyrine, J.; Gerl, C.; Rossel, C.; Richter, M.; Locquet, J.-P.; Smets, T.; Sousa, M.; Andersson, C.; Webb, D. J. *Appl. Phys. Lett.* **2010**, *96*, 212901.
(38) Chauhan, L.; Hughes, G. High resolution synchrotron radiation based photoemission study of the in situ deposition of molecular sulphur on the atomically clean InGaAs surface. *J. Appl. Phys.* **2012**, *111*, 114512.
(39) Dalapati, G. K.; Tong, Y.; Loh, W.-Y.; Mun, H. K.; Cho, B. J. Electrical and Interfacial Characterization of Atomic Layer Deposited High-κ Gate Dielectrics on GaAs for Advanced CMOS Devices. *IEEE Trans. Electron Dev.* **2007**, *54*, 1831−1837.
(40) Suh, D. C.; Cho, Y. D.; Kim, S. W.; Ko, D.-H.; Lee, Y.; Cho, M.-C.; Oh, J. Improved thermal stability of Al_2O_3 /HfO_2/Al_2O_3 high-k gate dielectric stack on GaAs. *Appl. Phys. Lett.* **2010**, *96*, 142112.
(41) Marchiori, C.; El Kazzi, M.; Czornomaz, L.; Pierucci, D.; Silly, M.; Sirotti, F.; Abel, S.; Uccelli, E.; Sousa, M.; Fompeyrine, J. Physical and electrical properties of scaled gate stacks on Si/passivated $In_{0.53}Ga_{0.47}As$. *ECS Trans.* **2013**, *58*, 369−378.